Mineral reactions during natural carbon sequestration in low-permeability rocks

Author: Lucila Dunnington

Advisor: Prof. Jay Ague

Second Reader: Zhengrong Wang

A Senior Thesis presented to the faculty of the Department of Geology and Geophysics, Yale University, in partial fulfillment of the Bachelor's Degree.

Abstract

As carbon sequestration becomes a more viable way to combat the rapidly growing environmental predicament caused by global emissions, study of natural phenomena is essential for understanding carbonation processes and the sequestration potential of rocks. The focus of this paper is on understanding how the introduction of CO_2 fluid in porous space results in the precipitation of carbonates, or the alteration of surrounding rock. If the carbonation reactions lead to large enough volume changes to crack the rock, more porosity would be produced inherently, thus facilitating the reactions. Alternatively, dissolution-reprecipitation reactions may replace preexisting minerals like plagioclase feldspar with carbonates without noticeable expansion or cracking. Either process would give distinct limitations on the storage potential of rocks selected for sequestration. The samples for this study are from the Brimfield Schist, northeastern Connecticut. The rocks underwent high-grade metamorphism during the Devonian Acadian orogeny. During the late stages of the orogeny under kyanite zone conditions, fluid infiltration occurred along fractures, which drove carbonation and hydration reactions in cm-scale alteration selvages. Carbonate minerals that precipitated include dolomite, magnesite, calcite, and some siderite. Four chemical maps of key points on three different thin sections were made using the electron probe, tracing Ca, Mg, Ti, O, C, Na, Al, Si, K, S, and Fe to test for dissolution-reprecipitation in the rock samples from the Brimfield gneisses. These maps came to show exceptional evidence for dissolution-reprecipitation occurring between pre-existing plagioclase

and precipitated carbonate phases. The outer margin of the plagioclase grains show depleted levels of calcium and aluminum in regions where calcite-dolomite, and small clusters of kyanite are growing. The liberated Ca is inferred to have reacted with CO_2 and other elements in the infiltrating fluids to produce calcite and/or dolomite. Likewise, the sodium levels in the same boundary regions increase substantially. There is little evidence for cracking or volume expansion around sites of reaction. The compositional chemical gradients and the position of these gradients relative to grain boundaries and areas of alteration mineral growth suggest that dissolution-reprecipitation does in fact dominate the propagation of carbonation reactions in feldspar.

Introduction

As levels of carbon dioxide in the Earth's atmosphere rise at alarming rates, it is apparent that the scientific community must take steps to study the ways in which large-scale climatic effects that could be proven harmful to humanity can be somehow prevented or controlled (e.g. Lackner, 2002). One such method proposed to reduce the mounting CO_2 in the atmosphere is to sequester the carbon dioxide in permeable rocks in the upper crust. A company in Norway (Statoil) at the Sleipner site in the North Sea has developed a process of injecting carbon dioxide into the fluid-filled pore space of sandstone. Their method was developed in response to a carbon tax the government has emplaced, making this system economically viable.

However, the use of sandstone for this particular process is questionable as a global solution, as these "saline aquifers" could leak CO_2 over time (Pacala, 2003). Alternatively, mafic rocks are abundant, their reaction with CO_2 is energetically favorable, and the solid product is inert and leak-proof.

At low temperatures and pressures, slow weathering of mantle peridotites leads to the formation of altered rocks rich in carbonate minerals, namely magnesite, dolomite and calcite. While the reaction is exothermic with negative ΔG, the time necessary for these reactions to take place is too long to be a feasible solution (Kelemen and Matter, 2008). So research now at Yale is focusing on how to manipulate conditions around mafic rocks, which occur in large volumes around the world, to increase the rate of their carbonation. One solution would be to try to make these reactions occur at depth so that the naturally higher temperatures and pressures of the system alter the kinetics to accelerate the reactions. The exothermic carbonation reactions would sustain a higher temperature with relatively little initial input energy.

Part of the problem in using mafic rock as opposed to sandstone, however, is the reduced permeability of the matrix. If the CO_2 cannot flow easily though the rock, it would be difficult to sequester the vast amounts of carbon desired for stabilizing global levels. One idea proposed is that the natural formation of carbonates in the solid rock will cause expansion, which will crack the dense surrounding rock, increasing reactive surface area (Kelemen and Matter, 2008).

Before the process initiates the exothermic reactions that could sustain the high temperatures needed, the fluid must attain a higher temperature through contact with deeper rocks. The fluid will be pumped down to a certain depth at which it will be able to react readily and quickly with the surrounding mafic material.

Currently, the focus of this study is on examining natural examples of carbon sequestration in order to make precise predictions of how mineralization of carbonates occurs. Such an understanding of the specifics of the natural process would facilitate an anthropogenic reproduction of a sequestration setting. I am examining thin sections from a unique rock sequence, the Brimfield Formation, in eastern Connecticut, which underwent fracturing and influx of CO_2-rich fluids during the Acadian orogeny at 380-390 Ma (Ague, 1995). These rocks provide a natural laboratory for studying how CO_2-rich fluids infiltrate and react with low-permeability mafic and intermediate rocks of the crust. CO_2 was deposited mostly as magnesite and dolomite, two key mineral targets of sequestration of anthropogenic carbon.

Petrography forms a major part of the study. I have identified minerals and described the abundance, appearance and grain boundaries of crystals that have formed in the altered rocks. I have also recorded mineral associations in the various carbonated regions surrounding the carbonate veins. With the reaction process

approach, one can determine what reactions have taken place (Ague, 1994). It was critical to chemically map the CO_2 infiltration fronts preserved in thin section. Mapping of C, Mg, Al, and other key elements was done with the field-emission gun electron probe microanalyzer (FEPMA) at Yale. This instrument allowed resolution of CO_2 infiltration pathways along grain boundaries and cracks from the centimeter scale down to several hundred nanometers. We hypothesized that infiltration required coupled mineral dissolution-reprecipitation (e.g. Putnis, 2002; Putnis and John, 2010); the mapping tested whether the preserved carbonate metasomatism is consistent with this process.

Generally, the reactions given most attention resulting from mass transport occur around grains, or in fluid-filled cracks or pore spaces. Another, often neglected, form of transport is intracrystalline diffusion. In many cases, when fluid-flow through porous rock is fast, this type of diffusion is slow enough to be ignored. However, when fluid-mediated transport is slow, for instance in rocks with low porosity, diffusion reactions are significant in influencing the chemical compositions of fluids and surrounding crystals. While intracrystalline diffusion alone is limited in its range of impact, studies suggest a coupled dissolution-reprecipitation replacement reaction causes extensive chemical exchange in a variety of crustal conditions (Putnis, 2002; Putnis and John, 2010).

Coupled dissolution-reprecipitation takes place when disequilibrium fluid contacts preexisting surrounding minerals. These minerals are then replaced by

ones in equilibrium with the fluid. The interface for the reaction advances beyond the boundary of the grain, and in its wake is an area of micro- or nanoscale porosity, filled with fluid, transporting reaction products outward and reactants inward (Putnis and John, 2010). The porosity is either a result of a net negative volume change in the replacement reaction, or slower rates of precipitation than of dissolution. In either case, it is because of this added porosity this process creates that it exceeds the alteration expectations (in speed and expanse) of solid-state intracrystalline diffusion. This coupled mineral dissolution-reprecipitation is an intriguing type of replacement process for geologic storage of carbon dioxide, because it increases the storage capacity of formations with the replaceable minerals.

The alternative reaction process would occur as pore space reaches maximum capacity with incoming fluid and crystal growth. Since hydration and carbonation reactions increase the solid volume of the material involved, enough stress could generate the fracture of the surrounding rock, creating new pathways for fluids to enter, and more surface area for reactions to take place. Evidence of this has been observed in mineral replacement experiments by Jamtveit et. al. (2009) and generally appears as cracks radiating from a newly crystallized alteration mineral, or concentric cracking around the older mineral. This sort of natural hydrofracture is also of interest to geologic sequestration studies, since it would reduce the expenditures of implementing human hydrofracture technology.

Thus far, the experiments run by Professor Zhengrong Wang as the lead PI, reveal that aluminum in the fluid may be key for catalyzing carbonation reactions. Since the field setting I studied also indicates coupled Al and CO_2 mass transfer, the comparison of the natural rocks and the experiments could be valuable. These rocks present a compelling and significant example of natural carbonation processes that should be fully understood before artificial simulation and larger scale application are implemented.

To summarize, a major goal of this study is to determine if the intrinsic porosity and permeability of the natural rock samples are sufficient to allow extensive carbonation during mineral reaction. If so, then C sequestration in natural rock formations may not require extensive hydrofracturing or other methods of porosity-permeability generation. Fossil fuels continue to be an overwhelmingly important present and future prospect for supplying the energy consumption of the world (Sheppard and Socolow, 2007). As long as they remain a major player, their problematic waste products must be handled in an appropriately safe and inexpensive manner.

Geologic Setting

The Brimfield Schist is part of the Merrimack Synclinorium, extending from northeastern Connecticut up to New Hampshire (Thomson, 2001). The samples were obtained from a 0.75x0.25km quarry near Willington, CT. Most of the exposed

rocks are gray or rusty colored, and were sedimentary and igneous rocks that formed schists and gneisses during the Devonian Acadian orogeny around 400 Ma (Thomson, 2001; Ague, 1995). The predominant granulite facies mineral assemblages in metapelites is sillimanite + plagioclase + quartz + garnet + cordierite + k-feldspar ± biotite ± spinel (Ague and Eckert, 2012). Quartzofeldspathic gneisses contain mostly plagioclase + garnet + orthopyroxene + quartz ± biotite ± clinopyroxene. Mineral assemblages in mafic gneisses are characterized by plagioclase + orthopyroxene ± clinopyroxene ± olivine ± biotite.

Thomson (2001) condenses the tectonic history of this region into three significant stages: in the first, the nappe stage, the region undergoes intense folding; then the second stage is an overturning of the thrust nappes, when 'peak' metamorphism occurred, between 362-369 Ma; and the third stage, the "dome stage," takes place as gneiss domes rise west of the synclinorium, and is characterized as a time of unroofing and cooling. The exact series of geologic events in this region is disputed, but evidence from multiple studies suggested a general 'anticlockwise' pressure-temperature (P-T) path (Winslow, 1994; Ague, 1995; Hames, 1989) More recently, Ague et al. propose a modified P-T path for this formation. This path corresponds petrologically to a sequence of plutonism, metamorphism, and exhumation (2012). In the first stage, the area is subjected to very high temperatures (~1000˚C) and minimum pressure of ~1.0GPa around 420-415 Ma, as evidenced by the presence of sillimanite pseudomorphs after kyanite, rutile needles in garnets, and antiperthite exsolution (Winslow, 1994 and Ague et

al., 2012). The appearance of cordierite and spinel suggest maintained high temperature to ultrahigh temperature (HT- UHT) conditions, while the rock was exhumed to pressure ~0.6 GPa. This was followed by cooling to ~800˚C at more or less constant pressure, during which time garnets and orthopyroxenes equilibrates in quartzofeldspathic gneisses. Temperatures decreased to ~600˚C but pressures increased to ~0.9GPa in the kyanite zone. Fractures that ultimately host the CO_2 infiltration fluid form in this zone; subsequent carbonate mineralization takes place in these fractures and in adjacent alteration selvages (Ague 1995; Ague 2012).

Methods

Thin sections had already been prepared and mostly polished by the time of this study. Backscattered electron imaging (BSE) as well as energy-dispersive scattering (EDS) and wavelength-dispersive scattering (WDS) were done with the JEOL JXA 8530F field emission gun electron probe microanalyzer (FEPMA), Department of Geology and Geophysics, Yale University. Some thins sections had to be repolished and recoated with carbon for FEPMA studies.

Significant features observed in thin section were recorded, such as crack propagation, grain dissolution, aluminosilicate formation (either as large feathers or in “fuzzy” boundaries), and the appearance of minerals such as cummingtonite or carbonate. The thin sections chosen, due to their exceptional expression of aluminosilicate formation, grain dissolution, and carbonate mineral proliferation

were JAQ-9-2, JAQ-18-51, and JAQ-14. Two areas of JAQ-14 were finally selected to produce maps, one area on JAQ-9-2 and one area on JAQ-18-51.

The hand sample from which thin section JAQ-18-51 was made is representative of vein-related fluid infiltration in the field area. The dark gneiss is uniform with flakes of biotite growing over the originally mafic matrix. Where there seems to have been a wide (at least 40 cm) fluid filled vein, there is an assemblage of carbonate phases (dolomite, magnesite, and ankerite appear most commonly), muscovite, almandine-rich garnets (3-5cm in diameter), and kyanite (up to 3cm in length) in a layer about 3cm thick on top of the hand sample (Ague, 1995). An alteration margin (selvage) of about 1 cm between the original rock and the vein is visible. A polarizing lens on a compound light microscope at magnification 25x shows the presence and abundance of cummingtonite (a metamorphic amphibole) and sodic biotites (together occupying ~5% of the thin section). The plagioclase grains are zoned around the contact boundaries of alteration minerals (such as the carbonates, biotites, and cummingtonite) but their twinning is not broken or deformed, suggesting chemical alteration; the most common form being a calcic center, and becoming more sodic towards the edges (Cannon, 1966). The carbonate minerals in this piece coincide with kyanite crystals, in terms of location and level of development. In this thin section, micron-scale, bright needles appear in garnet, which according to previous studies are dominantly rutile or ilmenite and indicate extreme P-T conditions for rock formation (Ague and Eckert, 2012). The particular region of interest of thin section JAQ 18-51, which was targeted for the electron

probe has an interesting area of remnant plagioclase grains surrounded by carbonate and other alteration material; it was selected to possibly investigate a stage of vein fluid infiltration of host-rock minerals. In this targeted area, 1.2x1.2 mm, aluminum, carbon, potassium, sodium, silicon, oxygen and sulfur were mapped using energy dispersive spectrometers (EDS), and carbon, calcium, iron, magnesium, and titanium were mapped with wavelength dispersive spectrometers (WDS).

The sample from which thin section JAQ 14 was made contains more confined, discreet regions of carbonate alteration. The dolomite and biotite are present, but the alteration rim is much shallower (~0.5cm) than that of JAQ 18-51, suggesting perhaps less contact with the chemical-rich fluid. In thin section, cummingtonite and biotites are also prominent in regions of extensive alteration of the original quartz and plagioclase. The first targeted area of this thin section, Map 1, provides another look at carbonate dissolution and reprecipitation around a silicate structure. In the 1.0x1.0mm area selected, EDS maps were made of Al, C, Ca, K, Na, oxygen, and Si; and WDS maps of C, Ca, Fe, Mg, and Ti. Map 2 of JAQ-14, 500x500 microns, provides an interesting view of the margin of dissolution between material in a fluid channel and wall rock. EDS maps were made of Al, C, Na, O, S, Si, and Ti; WDS maps were made of Mg, K, Fe, Ca, and C.

JAQ-9-2 rock sample has multiple sites of garnet growth, larger (2-4 cm) kyanite blades, magnesite, and pyrite on the exposed part of the rock. In thin section, the kyanite blades emerge out of altered plagioclase. The area for electron

probe mapping was selected to investigate the origins of such a spontaneous outgrowth. EDS maps of Al, C, Ca, Fe, K, O, Na, Si, and WDS maps of C, Fe, Mg, S, Ti were created to study the various chemical pathways that may have resulted in the surprising occurrence.

Once the areas of interest were rediscovered in the BSE image and point checks on the electron probe verified the major mineral and elemental pieces in the area of interest, the range was decided and set. Ca, Mg, Ti, O, C, Na, Al, Si, K, S, and Fe are the most relevant to this study and so were the major ones traced in the four maps created. The total time for processing the thin sections in the electron probe was close to 60 hours.

Results and Observations

Figure 1 is the BSE of Map 2 on JAQ-14. Areas having the same grayscale are in the same mineral group. The lighter, pointed areas of crystal growth that are interspersed in the dolomite and along the edges of the labeled plagioclase are biotites; these overgrow much of the remaining quartz and the northern edge of the labeled plagioclase. There are remnants of the quartz in the dolomite-rich area too, which have been heavily dissolved by the surrounding carbonate. The darkening of the grayscale in the labeled plagioclase, visible on its right and bottom edge, is the first indication of chemical alteration of the plagioclase minerals.

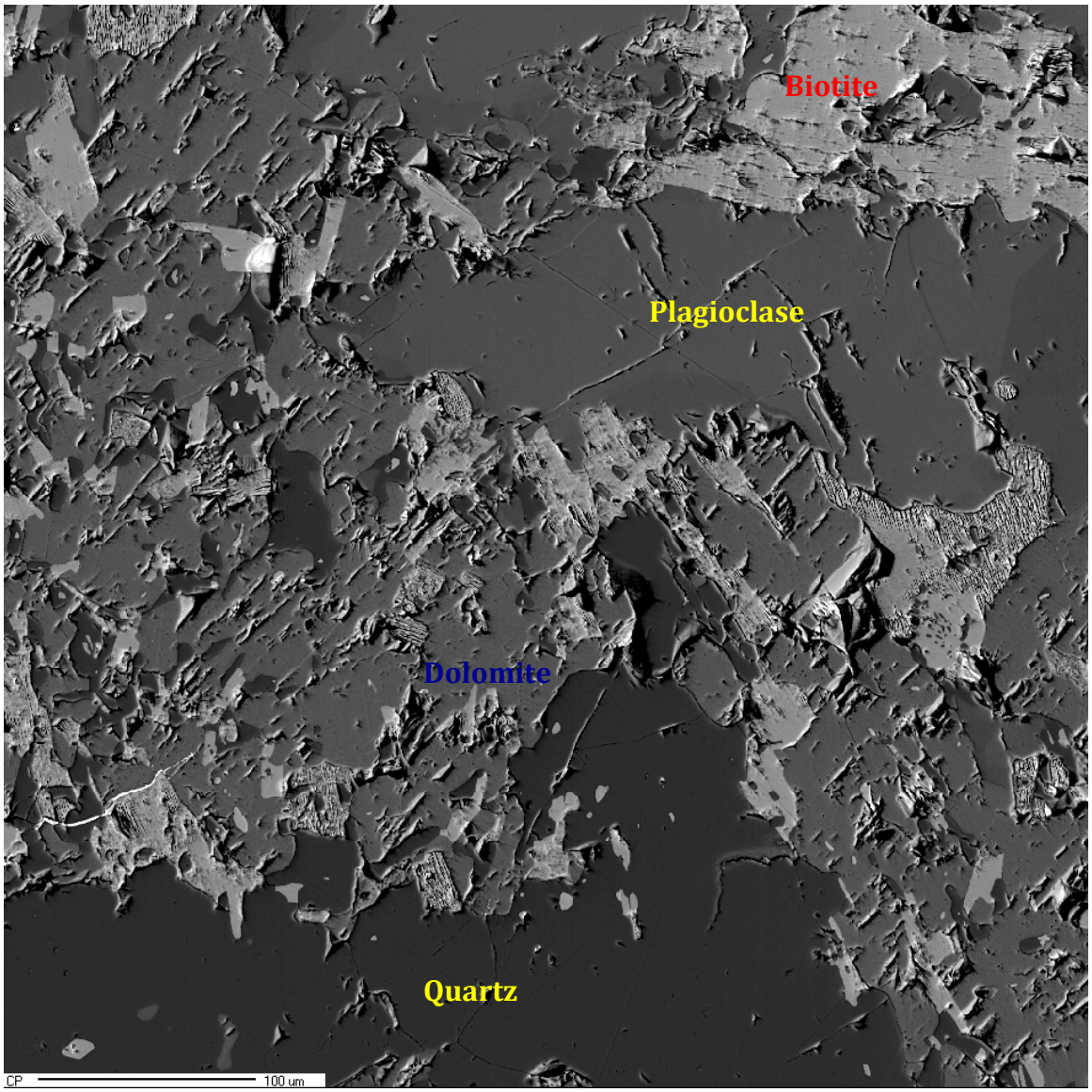

Figure 1: JAQ-14 Map 2, BSE, 500x500 microns. Quartz and plagioclase appear darker in the BSE due to their silicon content. In contrast, the lighter material contains significant amounts of iron and magnesium; further examination suggests these are biotite minerals. The material slightly lighter in appearance to the plagioclase, filling in around the plagioclase is Ca,Mg carbonate minerals, mostly dolomite. In this image alteration of the plagioclase is already visible in the darker areas on the east, west and south border of the labeled plagioclase.

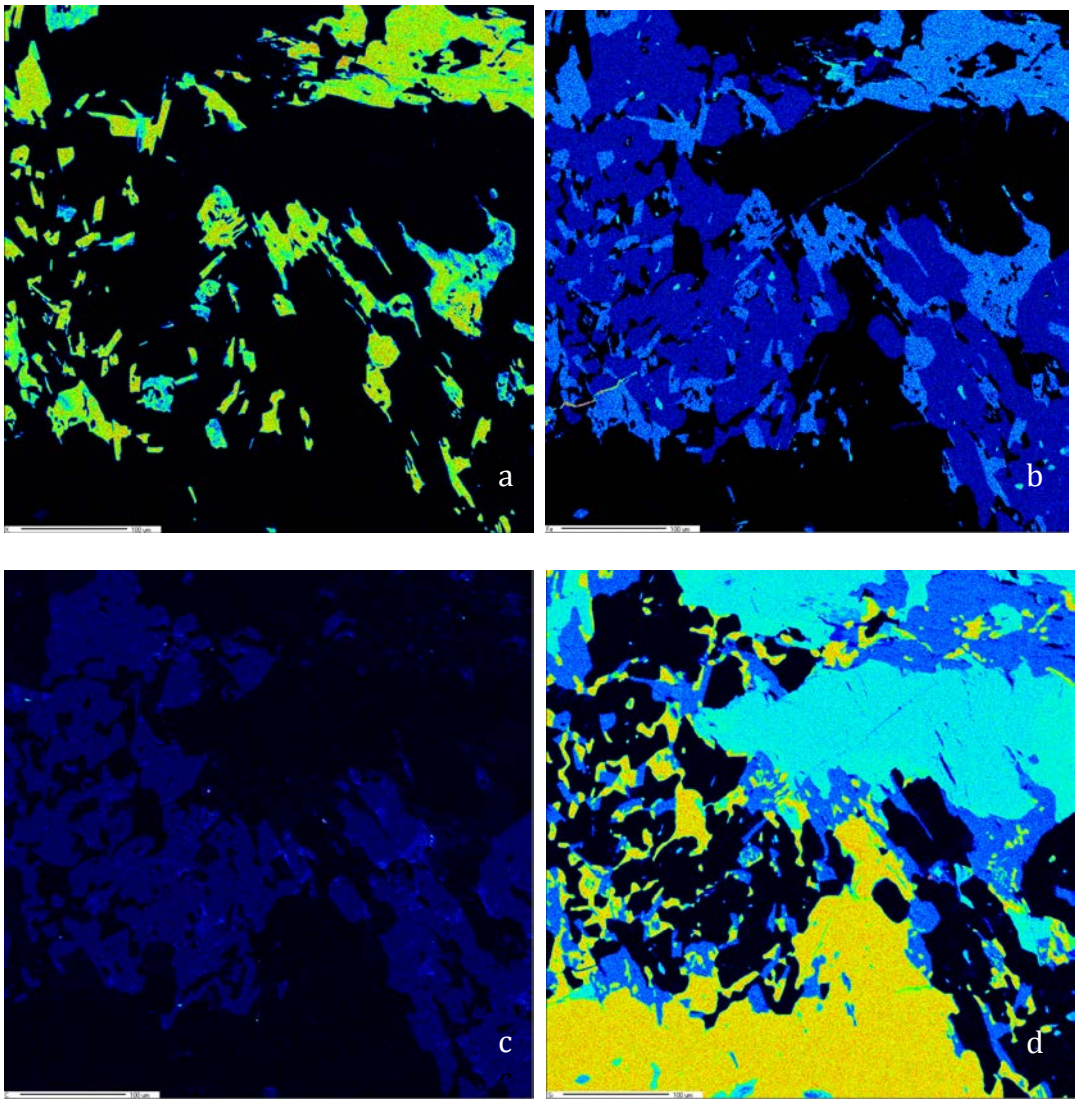

Figure 2: JAQ-14 Map 2, a. K WDS, b. Fe WDS, c. C EDS, d. Si EDS in 500x500 micron scale. The K and Fe maps show the extent of the biotite minerals more clearly. There is some evidence of crack and fill around the biotite minerals on the quartz and plagioclase grains. The Si and C maps distinguish the carbonate and silicate minerals more definitively. Regions between the identified biotite groups around the plagioclase are where dolomite growth is found.

In the images or figure 2, a close look at the potassium, silicon and iron maps trace the growth of the biotite. There is a sort of crack-fill propagation happening on the eastern side of the plagioclase and on the northern edge of the lower quartz region driven by the expansion of biotite crystals, similar in character to the

cracking recorded by the Jamtveit study (2009). However, this type of replacement is juxtaposed with the type that is found around the carbonate crystals. In figure 3, there is clearly alteration shading that extends from the dolomite phase carbonate, visible in the calcic plagioclase crystal. In the western tip of the Ca-plagioclase area, the shape of dissolution aligns with the dimensions of the adjacent dolomite crystal (the top arrow points to the area of calcium depletion mentioned).

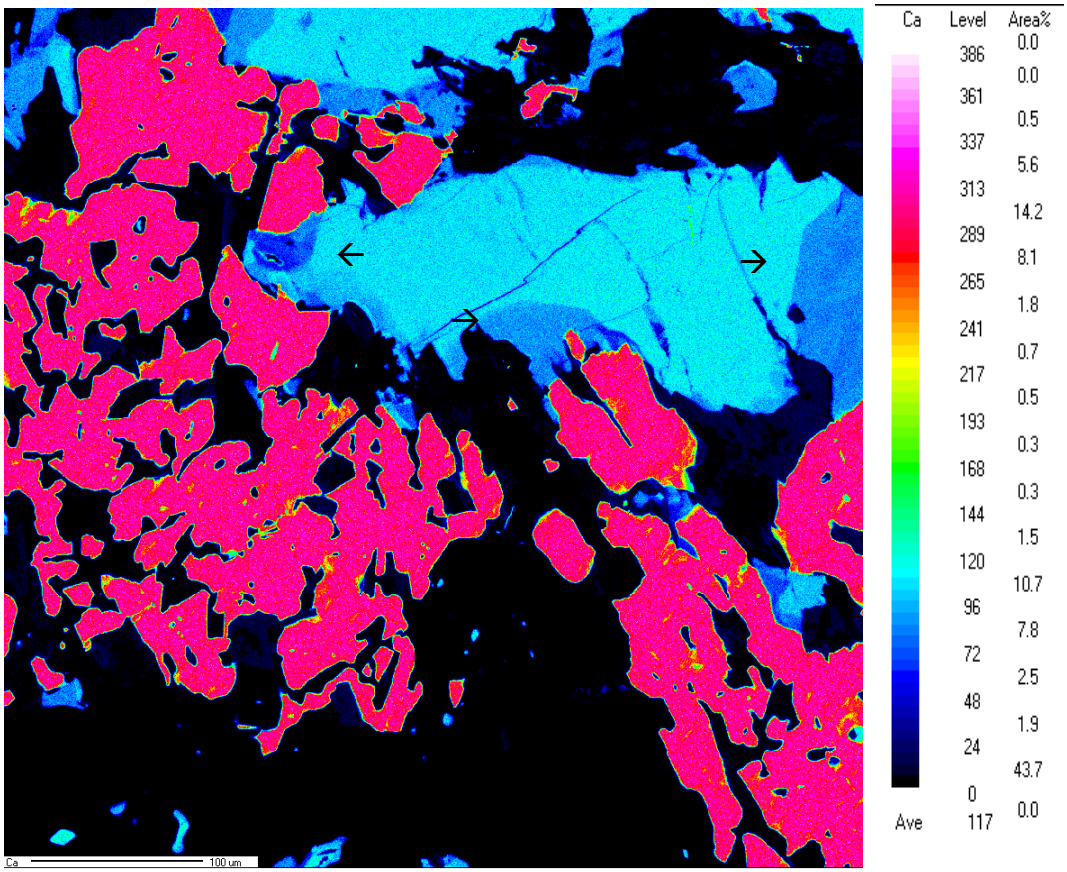

Figure 3: JAQ-14 Map 2, Ca WDS, 500x500 microns. Arrows indicate two central places of Ca depletion in the plagioclase. There are sharp edges around areas of depleted calcium in the plagioclase grains in the central and northern plagioclase grains. These regions can be compared to the regions in the plagioclase that border the biotites, which only show intracrystalline diffusion, appearing as a less definite and less penetrative region of calcium depletion. The scale to the right indicates level in ppt and the % of the image area occupied by each level of Ca enrichment.

The sharp region of elemental infiltration and the advancing front of dissolution are qualities of the coupled dissolution-reprecipitation replacement process (Ague, pending). (Simple intracrystalline diffusion can be observed in figure 3 as well. In the plagioclase grain near borders with the biotite, this simpler process of ion exchange appears as a lighter, fading gradient of Ca.) Similar examples of qualities of the dissolution reprecipitation mechanism are also visible on the southern edge of the plagioclase grain (the lower arrow) and the eastern side of the image (right arrow). The distinct areas of Ca depletion in the plagioclase grain are aligned with the upwards-extending dolomite crystals beneath it.

These dissolution gradients are also visible in the Al EDS map (fig. 4). However the dissolution manifests in the depleted regions of aluminum instead. The shape and extent to which the dissolution occurs is directly related to the corresponding dolomite growth in its vicinity. There is a more reliable correlation between aluminum depletion and carbonate growth (even though the relationship is not depicted as strongly in Al EDS as in the Ca WDS), since calcium depletion is also found, to a lesser extent and in a nebulous manner, on boundaries with biotite minerals.

The arrows on figure 5 (sodium EDS map) point to the areas where plagioclase was depleted in calcium and aluminum (seen in figures 3 and 4) and enriched in sodium.

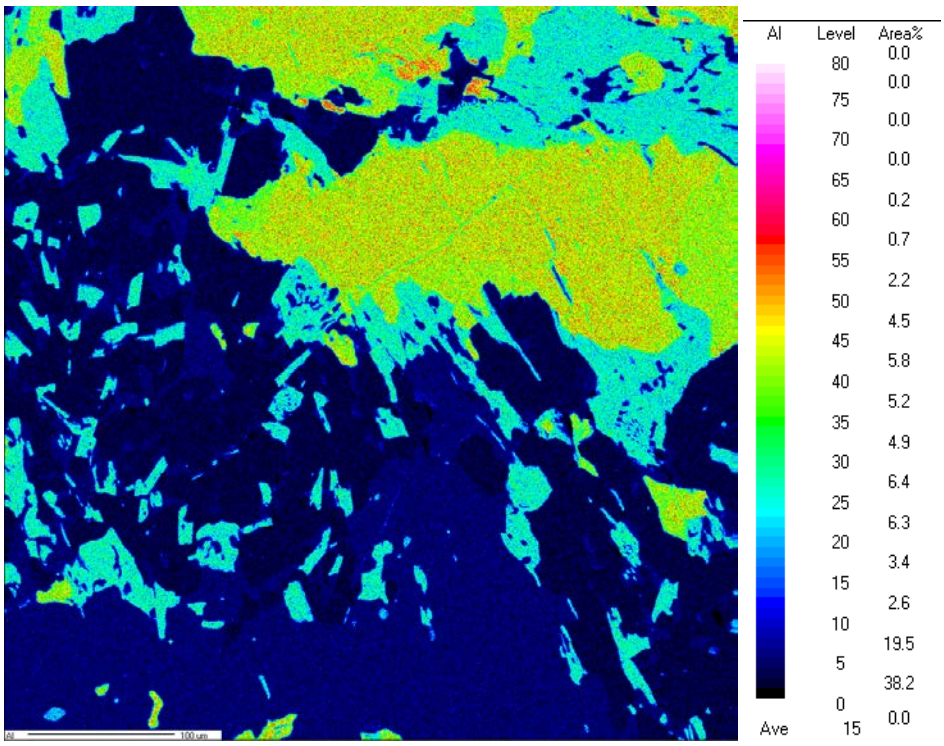

Figure 4: JAQ-14 Map 2, Al EDS, 500x500 microns.

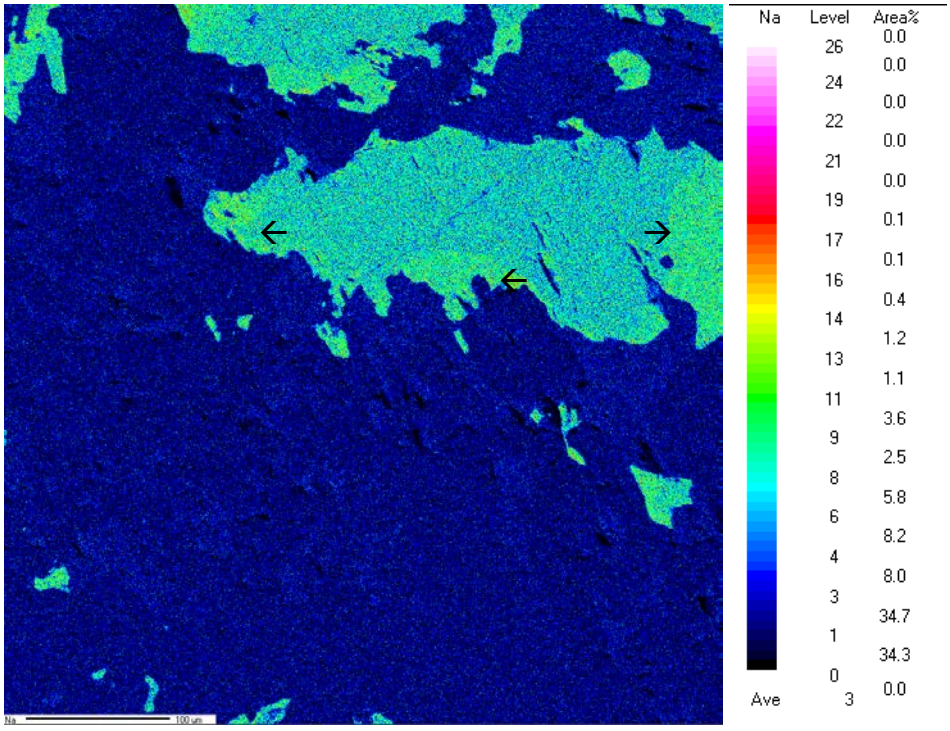

Figure 5: JAQ-14 Map 2, Na EDS, 500x500 microns. The above map shows that the levels of sodium are relatively higher in those regions shown to be depleted of Ca in figure 3.

Figures 1-5 give interesting insight into the nature of the physical and chemical reactions in and around Ca-plagioclase, a very prevalent mineral in various low-permeability rocks, in the presence of natural carbon sequestration. The cracking and filling found around some examples of biotite growth do not seem to propagate to the extent that one would expect in a large-scale replacement model in this sample.

The next map (figures 6-7) depicts a Ca-plagiolcase peninsula structure reaching out from the upper left corner. The Ca map (fig. 7a) shows similar Ca depletion as seen in figure 3, except more extensive, completely surrounding the pieces on calcic plagioclase, separating the calcic grains from the outermost region of variant carbonate growth (dominating the lower and right-side part of the images; blue regions of 7b). In the Na-plagioclase region (sodium map not pictured here), there are multiple blades of cross cutting muscovite minerals which also grow into the carbonate region.

JAQ 14 Map 1 (Fig. 6) provides an interesting image also of the distribution of various carbonate phases relative to one another. Mg pervades all of the carbonate mineralization on the image, but it is typically found coupled with either Ca or Fe. The pattern of carbonate formation rises a couple of questions that concern the study of natural sequestration: where do these ionic constituents (iron, magnesium, and calcium) come from; and is there any reason for their spatial arrangement, relative to the plagioclase minerals present in this selection?

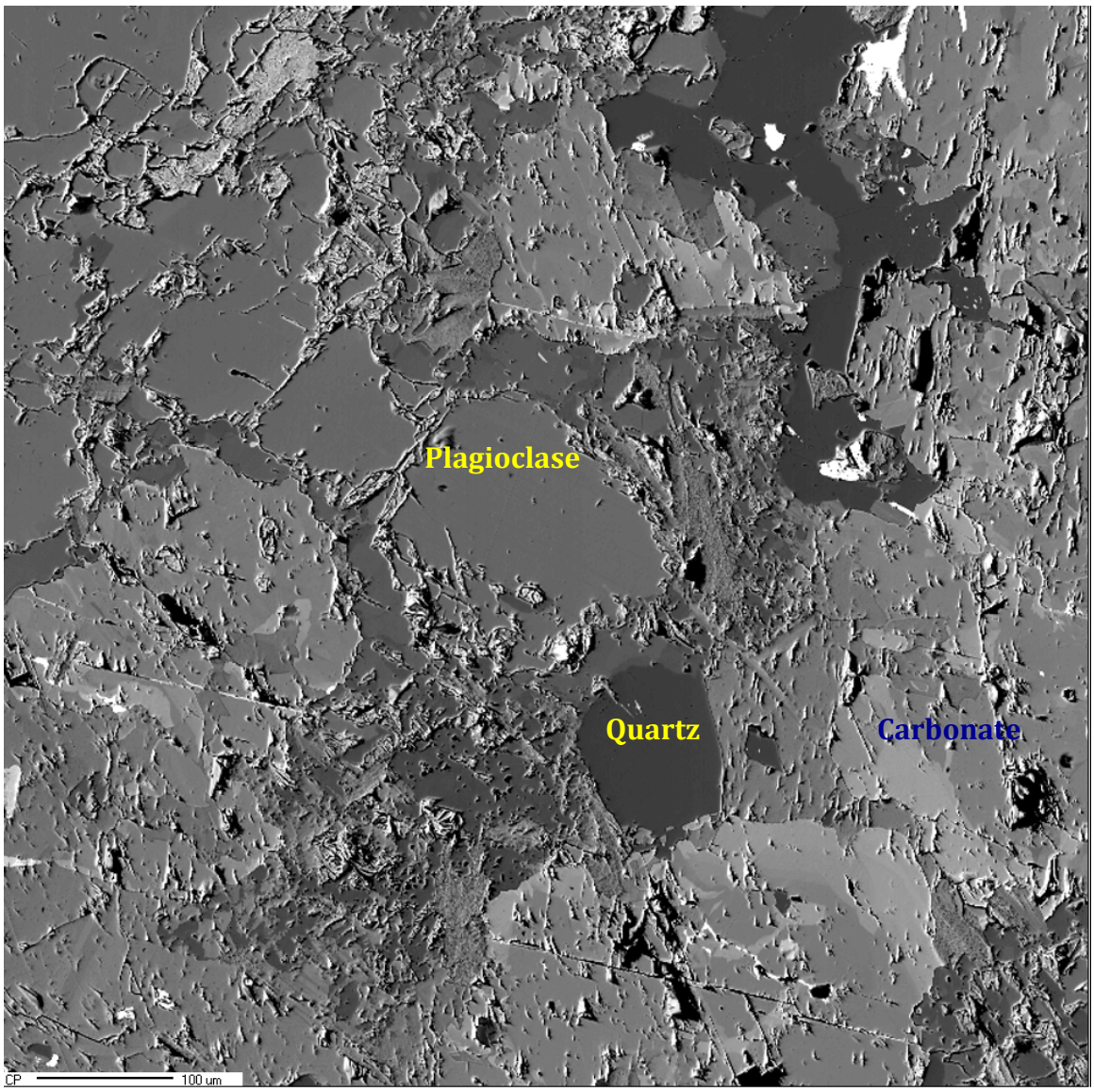

Figure 6: JAQ 14 Map 1, BSE, 1.0x1.0mm. The quartz minerals once again appear the darkest, and plagioclase minerals appear as the next darkest regions of this image. There is a wide range of grayscale for the carbonate minerals because here there is a mix of Mg, Ca, and Fe- carbonate minerals around the calcic plagioclase peninsula labeled above. More mica has evolved in the plagioclase surrounding the peninsula between the calcic plagioclase and the carbonate minerals.

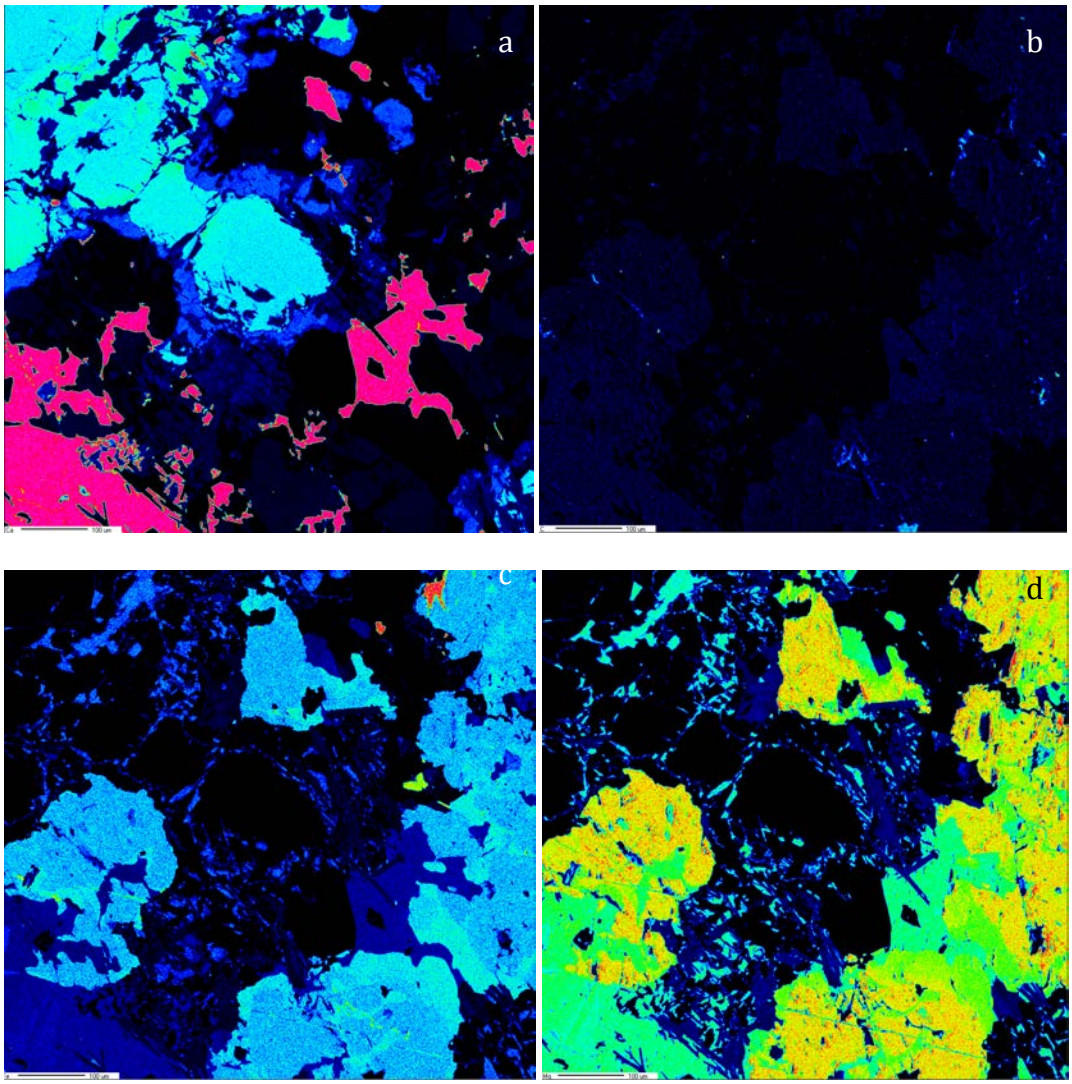

Figure 7: JAQ 14 Map 1, a. Ca WDS, b. C WDS, c. Fe WDS, d. Mg WDS, 1.0x1.0mm. The Ca, Mg, and Fe maps together give a layout of the distribution of carbonate minerals in the region around the plagioclase. Regions of higher calcium content appear in the bottom left corner, and tightly between areas with the highest iron level. Mg increases with increasing iron generally, but will deplete marginally where Fe content is at the next highest level.

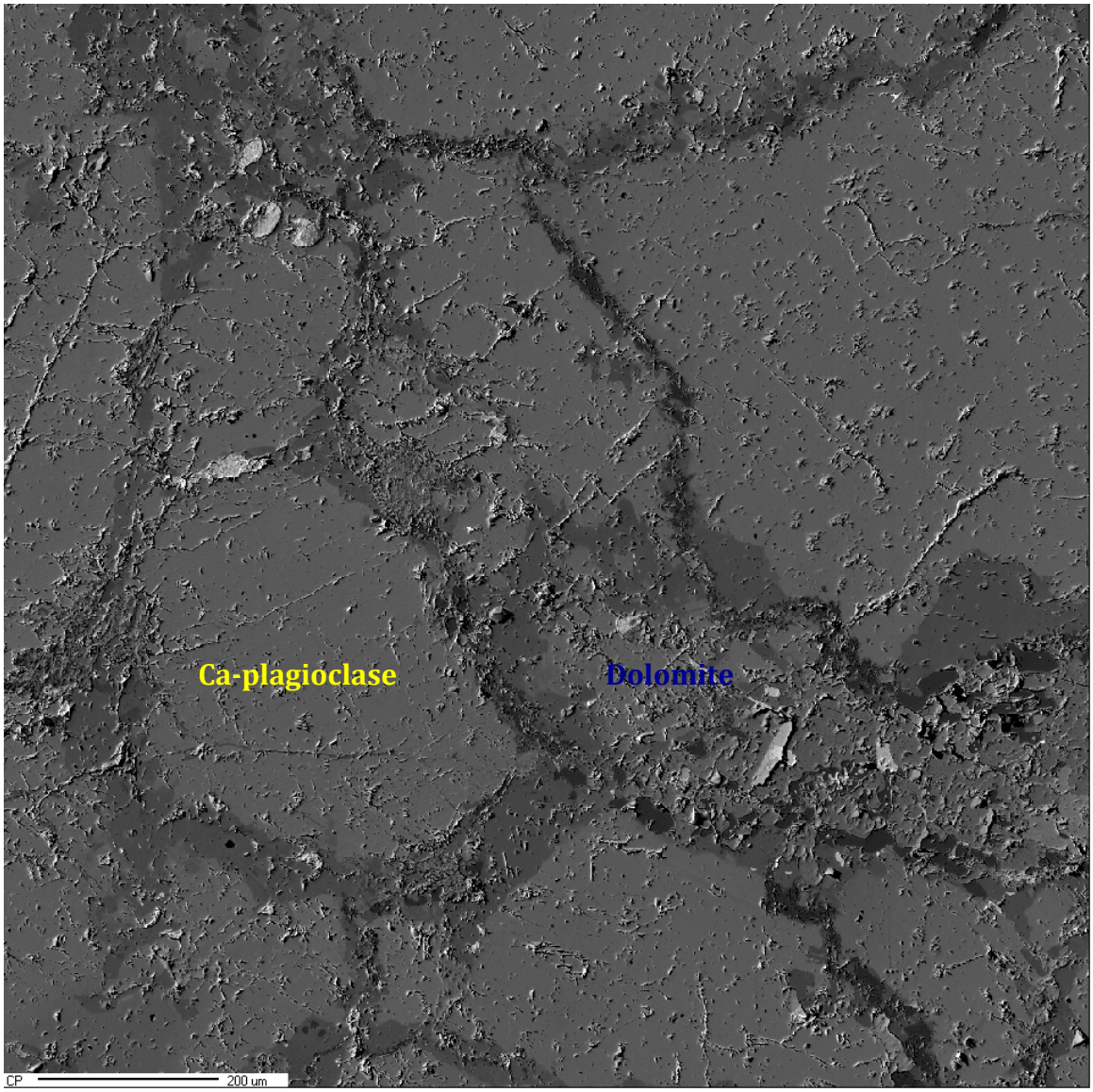

Figure 8: JAQ-18-51 Map 1, BSE, 1.2x1.2 mm. Calcic plagioclase appears as the color of the labeled grain. The slightly darker material surrounding these calcic grains is sodic plagioclase. The material with rougher texture between the two Ca-plagioclase grains on the right side of the image is dolomite. Though difficult to visually distinguish from the plagioclase in the BSE image, figures 9 and 10 provide adequate visual contrast for tracking the dolomite as it migrates through the Na-plagioclase conduits. The darker material in the Na-plagioclase is also discussed later, and featured more prominently in figure 12.

The FEPMA images of JAQ-18-51 show a later stage of replacement, in which the older plagioclase is completely surrounded by conduits of replacement mineral. Dolomite and magnesite carbonate phases occur most prominently in the lower right side of the map, but also have developed in discreet areas along the diagonal conduit of Ca-depletion extending northwest from the main section of carbonate mineralization (as is shown in the Ca and Mg images, fig. 9 and 10 respectively).

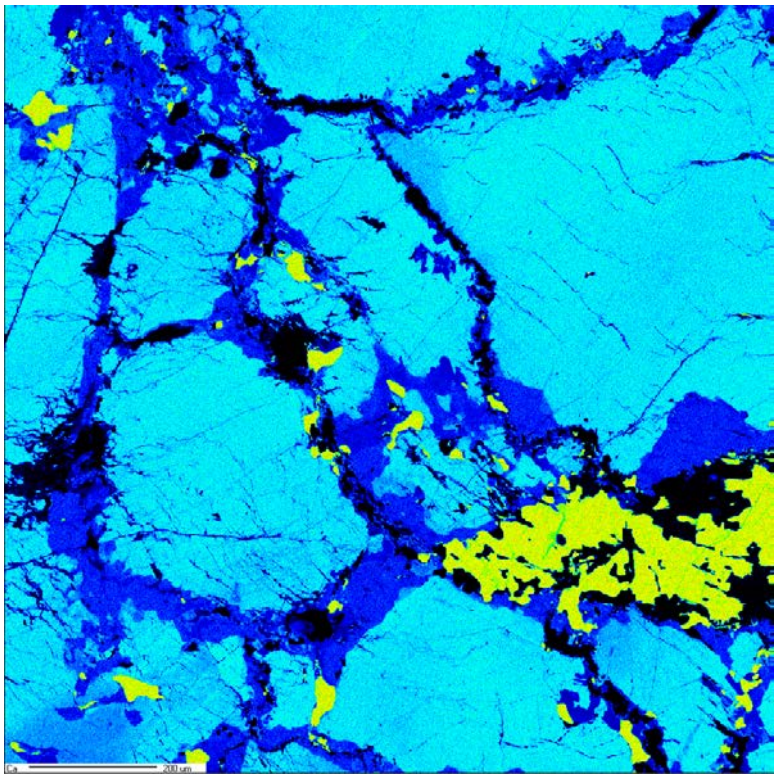

Figure 9: JAQ-18-51, Ca WDS, 1.2x1.2 mm. The bright yellow on this image show the distribution of Ca-carbonate (mainly in the form of dolomite) across the area of this selection. A closer inspection of this image reveals more intense Ca depletion in plagioclase regions surrounding the dolomite crystals, positioned in the Na-plagioclase pathways (This extent and alignment of this depletion is comparable to the qualitative observations made with figure 3).

Furthermore, in the Ca image, areas of Ca-plagioclase adjacent to the conduits are still in the midst of coupled dissolution-reprecipitation. The pointed corner of the large eastern plagioclase grain is being depleted of calcium and enriched in sodium (Fig. 11a). Similar depletion-enrichments are visible in the bottom left corner of the image, where another sodic conduit is being formed.

The sodium-rich plagioclase conduits are often inlaid with a stripe of "fuzzy" material, which appears bright red-orange on the Al map (figure 12). The same color signature is found on the kyanite blades of a later map (Fig. 13e). This aluminosilicate composition occurs in the sodic plagioclase regions.

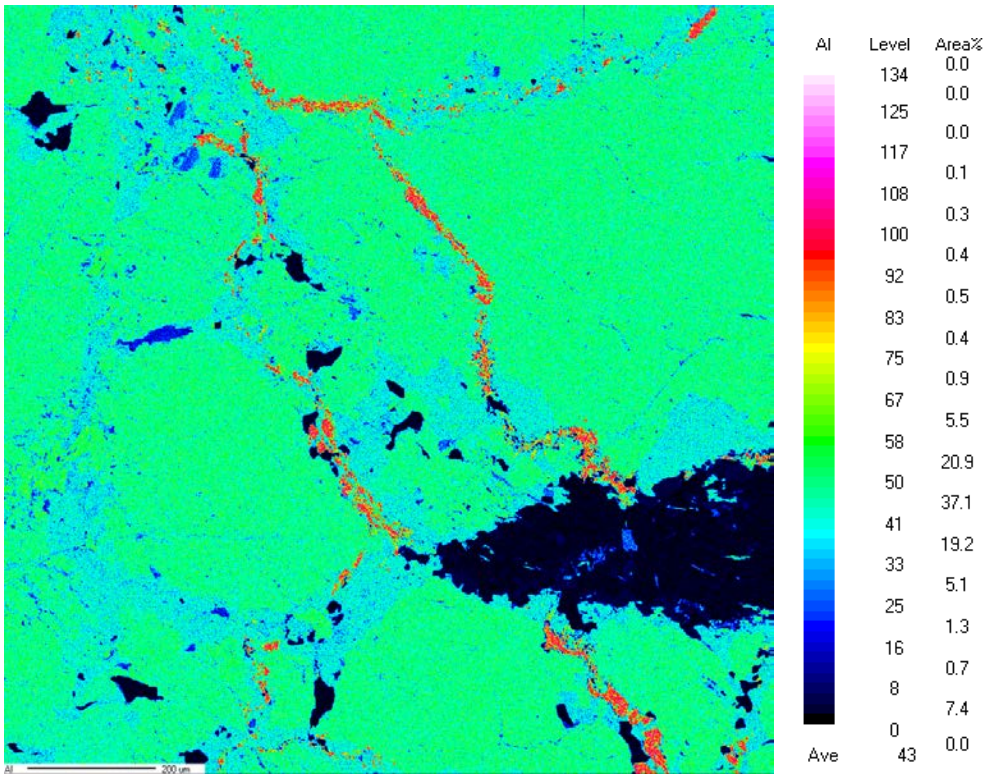

Figure 10: JAQ-18-51 Map 1, Al EDS, 1.2x1.2 mm

The appearance of newly formed minerals such as muscovite, kyanite and the upwards- migrating dolomite crystals are restricted to the replacement pathways defined by high sodium content in plagioclase. The cracking that has resulted from the growth of the micas (showing a similar behavior in JAQ 14 Map 2, Fig. 2a) is thus a consequence of the initial Ca-plagioclase to Na-plagioclase replacement. Furthermore, there is no evidence in the images here (8-12) of the concentric cracking of pre-existing material and/or filling-in of substantial amounts of replacement material in or around the major grains as has been described by Jamtveit (2009) or Putnis (2007).

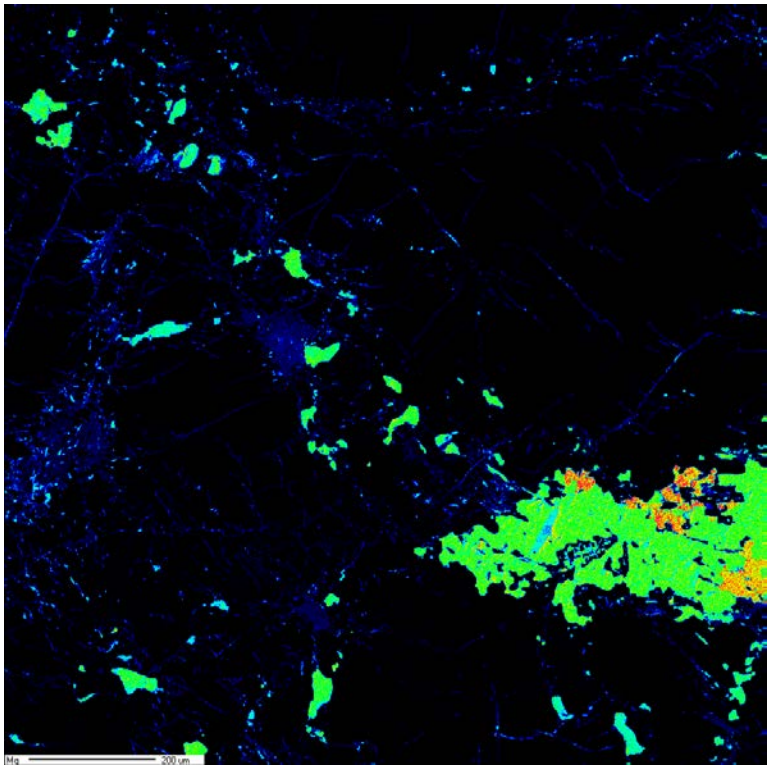

Figure 11: JAQ-18-51, Mg WDS, 1.2x1.2 mm. This image coupled with figure 9 shows the migration of dolomite crystals upwards from the main dolomite body to the northwest corner along the Na-plagioclase pathways.

a.

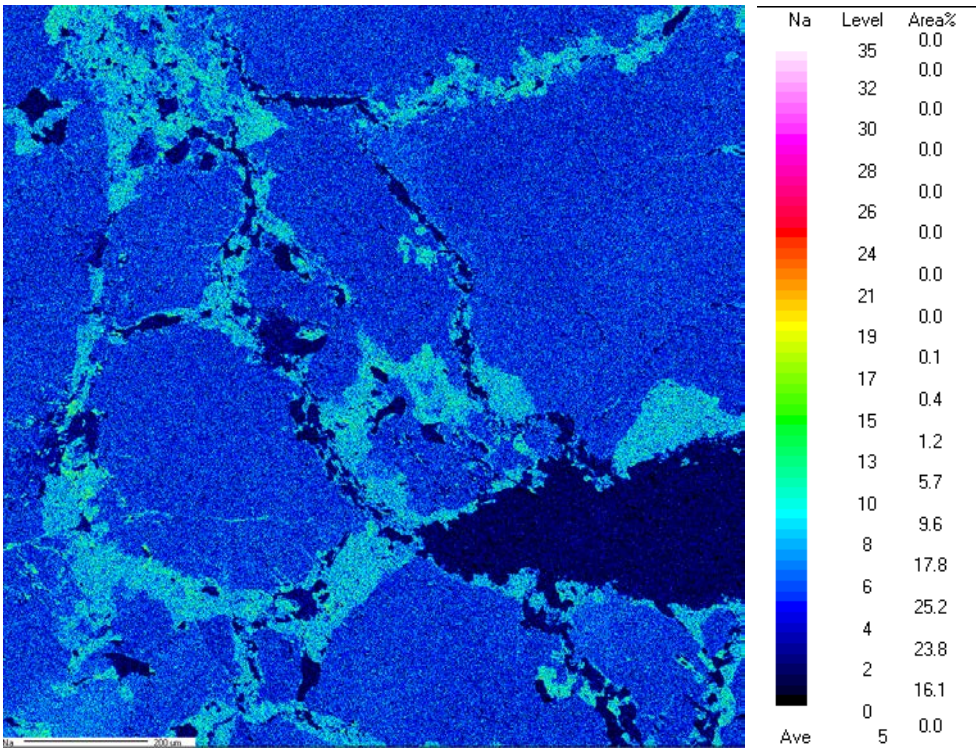

b.

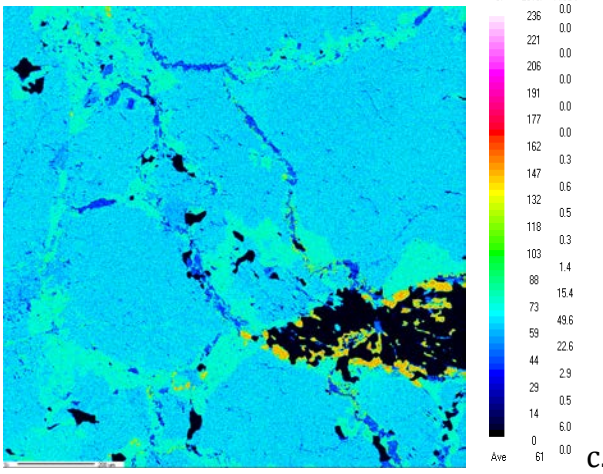

c.

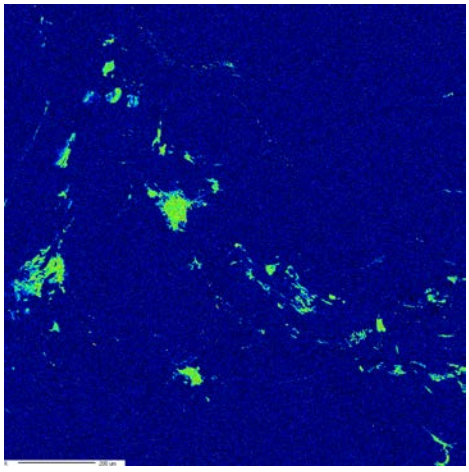

Figure 12: JAQ-18-51 Map 1, a. Na EDS, b. Si EDS, c. K EDS, 1.2x1.2 mm. 11a illustrates the higher Na content in the replacement pathways. These pathways converge around the dolomite section of the image, and host the other alteration minerals that have evolved. 11b distinguishes between the silicate minerals found on this image. The Ca-plagioclase has a lower Si level than the surrounding Na-plagioclase. Additionally, the aluminosilicate (identifiable on figure 12) appears much darker and restricted to the Na-plagioclase pathways. Quartz appears bright yellow on 11b as well, and is mainly

aggregated around the dolomite body. 11c accentuates the muscovite growth in the Na-plagioclase that cracks and fills on some surfaces of the Ca-plagioclase.

Figures 13 and 14 give a view of typical minerals that form along the veins of the studied rocks. It is typical to find, in the same vein, and almandine-rich garnet, kyanite blades and dolomite in proximity. All of this material new to the original mineral assemblages of the Brimfield schist occurs on a Na-plagioclase background the uniformity of the Na-plagioclase and the other minerals present suggest the ionic constituents of the infiltrating metasomatic fluid. In figures 13 and 14 below, the sheet-textured regions that correspond to peaks of K and Al are muscovite minerals forming to the left of the carbonate mineral region labeled.

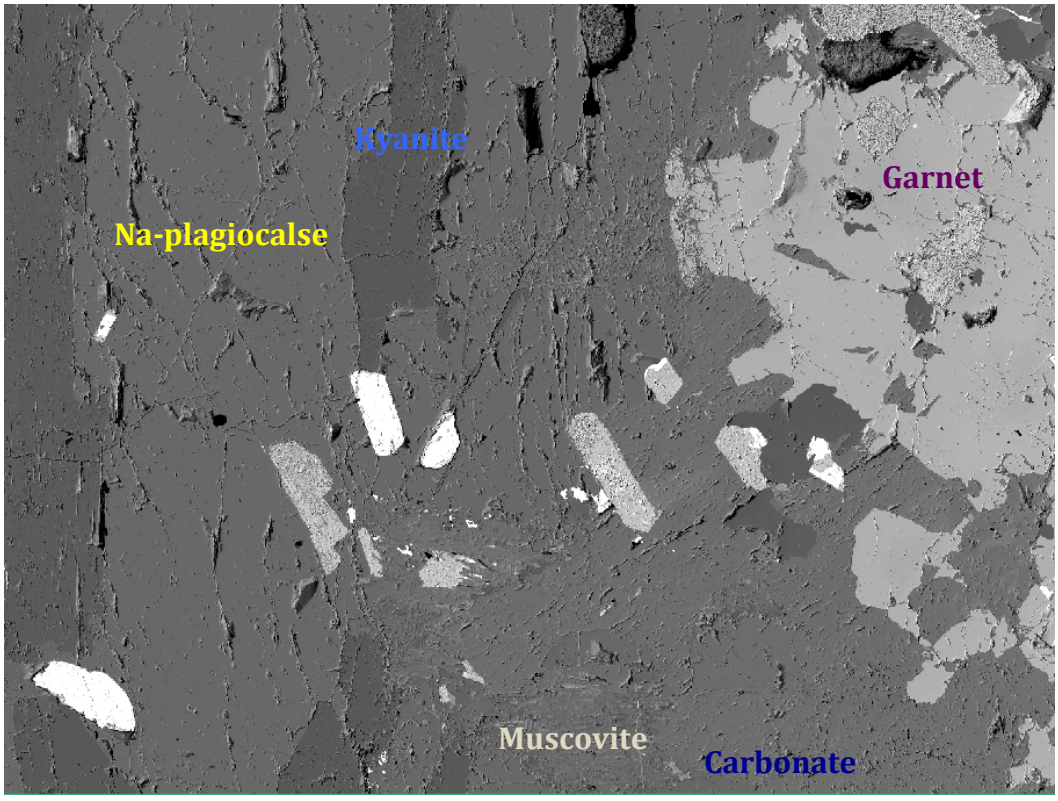

Figure 13: JAQ 9-2 Map 1, BSE, 1.9995x1.5 mm. In this image, there are a couple of new minerals that appear. Garnet forms the lighter mass in the upper right region labeled. Below that is a region of carbonate mineralization. A new sheetlike texture to the left of the carbonate label is chemically and

morphologically consistent with muscovite mineral compositions. The darker vertical blades found in the Na-plagioclase region on the left-hand side of the map are kyanite minerals (Al_2SiO_5). The other bright minerals that appear as long diagonally aligned rhombohedrals in this 2D image are ilmenite and rutile crystals.

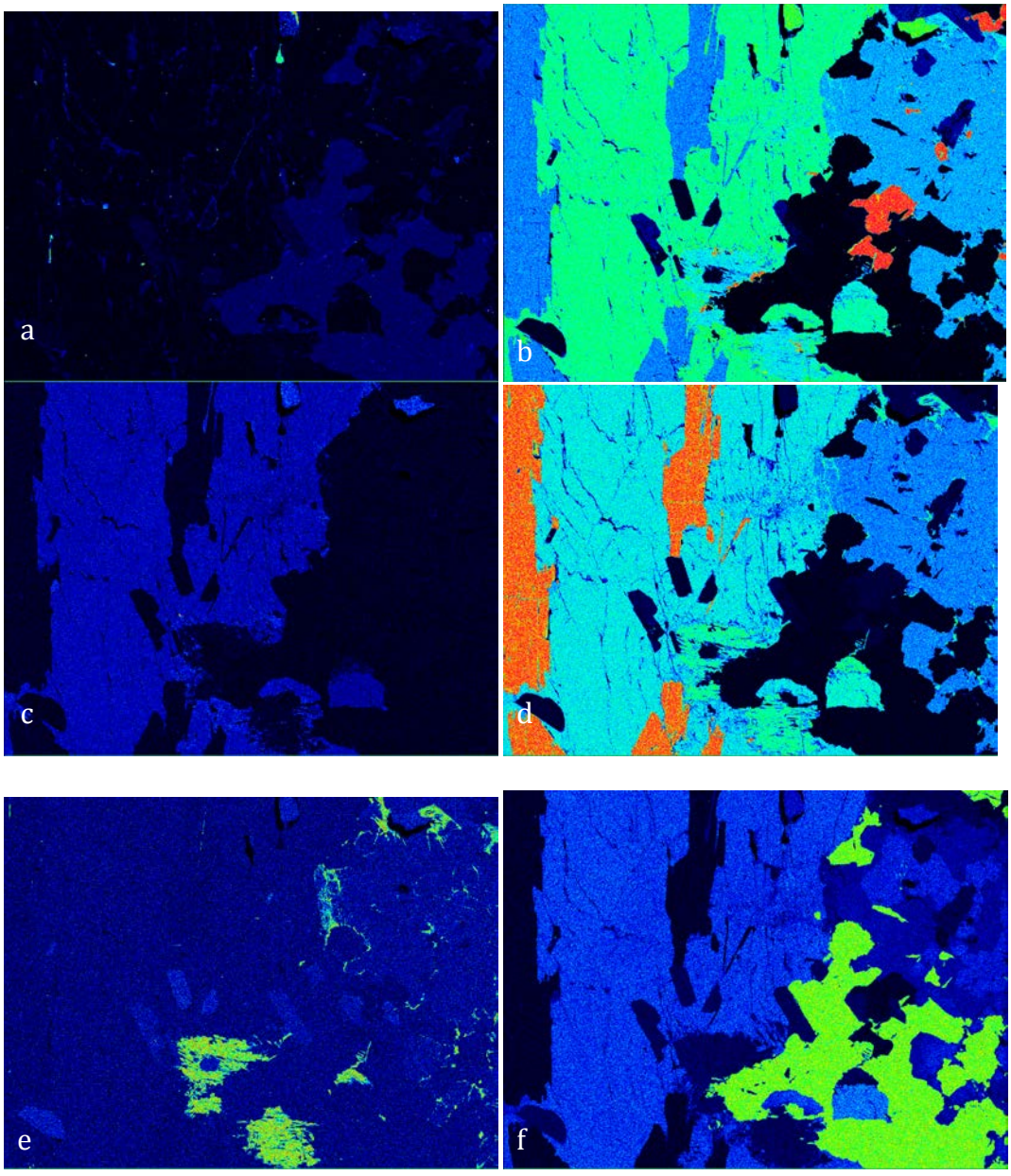

Figure 14: JAQ 9-2 Map 1, a. C EDS, b. Si EDS, c. Na EDS, d. Al EDS, e. K EDS, f. Ca EDS, 1.9995x1.5 mm

Discussion

The orientation and gradients of various elemental indices (Si, Ca, Al, Na) in the FEMPA images above (e.g. Fig 3-5, Fig. 9, Fig. 13-14) suggest that rather than producing and propagating cracks by reaction-driven expansion, discreet areas on preexisting minerals (i.e. Ca-plagioclase) off vein fronts are chemically altered by metasomatic fluid, containing high concentrations of ionic Na, Si, and K. The sharpness of the reaction front (e.g. figure 3) is characteristic of coupled dissolution-reprecipitation reaction (Ague, pending). Elemental constituents of a calcic plagioclase such as Ca dissolve into solution and are replaced by Na and Si from the metasomatic fluid, flowing through pore space or small (cm scale) selvages in the rock body. Figures 10, 11 and 12 demonstrate the extent to which coupled dissolution-reprecipitation may advance the reaction interface through a preexisting mineral matrix. Significant replacement is visible in the absence of cracking in these figures.

A generalized reaction describing the replacement is as follows:

$$1.5\ SiO_2 + CaAl_2Si_2O_8 + Na^+ + H^+ \rightarrow NaAlSi_3O_8 + 0.5\ Al_2SiO_5 + Ca^{2+} + 0.5H_2O$$

This recurring calcic plagioclase to sodic plagioclase reaction seems to precede any other chemical transfer or alteration to the original plagioclase grain. In figure 4, 7, and 11, the dolomite fronts are separated from the original Ca-plagioclase by the

intermediary zone of Na-enriched plagioclase, suggesting that carbonate growth is preceded by this preliminary dissolution-reprecipitation replacement, rather than a crack and fill type propagation.

Thus there is a correlative relationship between this initial chemical transfer and the carbonation reactions that come afterward. The conduits widening at the dolomite body in Figure 11a suggest the initial conversion to sodic plagioclase is essential to the progression of the carbonate minerals growth. The Ca dissolved out of the original plagioclase may also play a vital role in calcic carbonate mineral formation, if Ca ions that produce $CaCO_3$ or $MgCa(CO_3)_2$ come mainly from the dissolved Ca-plagioclase mineral. The source of the iron and magnesium for the growth of Fe,Mg- carbonate minerals is either the natural concentration of the infiltrating metasomatic fluid or products of past breakdown of orthopyroxenes previously a part of the rock's mineral assemblage.

The aluminosilicates that accumulate are also a product of the above reaction. The extra aluminum freed by the calcic to sodic plagioclase conversion combines with free quartz to produce the new mineral. This is also illustrated by the reaction above. Ca is removed, Na is added, and there is an excess of Al left over that makes kyanite. The Ca could in turn combine with carbon dioxide from the infiltrating fluids to produce carbonate minerals (calcite, dolomite). If the calcium ions released in these reactions contribute to in the formation of the calcium component of the dolomite. There remains the question of where the Mg and Fe in

the other carbonate minerals originate. The answer is uncertain; such ions could exist from the breakdown of discreet, pre-existing minerals, such as orthopyroxene and olivine. However, magnesium and iron ions might simply occur in the fluid solution.

The isolated regions of K attributed to outgrowths of micas most likely form from the breakdown of the calcic plagioclase, as well, in the following manner:

$$1.5\ CaAl_2Si_2O_8 + K^+ + 2H^+ \rightarrow KAl_3Si_3O_{10}(OH)_2 + 1.5\ Ca^{2+}$$

Evidence for cracking is seen around the micas in some cases, but the resultant cracking does not propagate more than ~10 microns from the contact region, and diffusion across the newly formed surface area does not constitute a significant amount of mineral replacement. However, this reaction does yield more ionic calcium that could again contribute to the formation of calcic carbonate minerals.

The figures suggest that the expansion cracking mechanism is not a predominant replacement model for the type of plagioclase replacement reactions that take place in this mineral assemblage. Rather, the coupled dissolution-reprecipitation process seems to correspond to the mineral behavior observable on the electron probe images. This process will have to be studied more for accurate carbon dioxide storage capacities to be calculated once geologic storage operations are initiated on a larger scale. Since reactions with carbonated fluid penetrate the

rock beyond natural porosity, the viability of low-porosity, low-leakage geologic formations can be explored as a prominent storage option for carbon emissions.

Summary

Various examples of plagioclase replacement indicate that dissolution-reprecipitation rather than fracture due to reaction-expansion is the main process that facilitates CO_2 infiltration and mineralization in the studied rocks. Although the carbonation of rocks is still dependant on available surface area on which to have reactions take place, this study shows that coupled dissolution-reprecipitation allows carbonated fluid to react with material past the wall rock in immediate contact with the veins, selvages or porous space. Thus, the amount of CO2 that can be added exceeds the initial porosity, increasing the storage potential of rocks with lower initial porosity.

The conditions of infiltration in the case of the Brimfield Schist are more extreme (temperatures ~600˚C and depths over 20 km) than those envisioned for industrial-scale sequestration in the shallow crust. It remains to be determined if dissolution-reprecipitation is a viable mechanism at such low P-T conditions, but this study has shown that this form of replacement needs to be considered and tested in the less extreme geologic setting. With more study into the nature of these reactions, the storage capacity of varying low-porosity rock types can be evaluated more carefully for the advancement of geologic carbon sequestration methods.

Acknowledgements

This study would not have been possible without the generous support provided by a Von Damm Fellowship, which funded the chemical maps. I also offer great thanks to Professor Jay Ague for careful teaching, advising and mentoring throughout the process. Thanks to Professor Zhengrong Wang and Qui Lin for assisting me in the lab this past summer, and allowing me to participate in the excitement of the experiments. Ague and Wang gratefully acknowledge support from Department of Energy grant DE-FOA0000250. I kindly thank Jim Eckert for his time and wisdom while assisting me with the field-emission gun electron probe microanalyzer (FEPMA). I would also like to thank DUS Dave Evans, and all the G&G graduates and undergraduates for their discussions and enthusiasm.

References Cited

Ague, J.J. (1994) Mass transfer during Barrovian metamorphism of pelites, south-central Connecticut, II: Channelized fluid flow and the growth of staurolite and kyanite. *American Journal of Science* **294**, 1061-1134.

Ague, J.J. (1995) Deep crustal growth of quartz, kyanite, and garnet into large

aperture, fluid-filled fractures, north-eastern Connecticut, USA. *Journal of Metamorphic Geology* **14**, 299-314.

Ague, J.J., Fluid Flow in the Deep Crust. *In* The Crust (ed. R.L. Rudnick), vol 3., *Treatise on Geochemistry*, 2nd Edition, (eds. H.D. Holland and K.K. Turekian), Elsevier, Oxford (accepted pending revision).

Ague, J.J. and Eckert, J. O., Jr. (2012) Precipitation of rutile and ilmenite needles in garnet: imlications for extreme metamorphic conditions in the Acadian Orogen, U.S.A.: *American Mineralogist* (in press)

Ague J.J. , Eckert J.O., Chu X, Baxter E.F., and Chamberlain C.P. (2012) Discovery of an ultrahigh-temperature metamorphic blister in the Southern Acadian Orogen, USA. (draft)

Benisek, A. Kroll H., and Cemic L. (2004) New developments in two-feldspar thermometry: *American Mineralogist* **89**, 1496-1504

Cannon, R. T. (1966) Plagioclase zoning and twinning in relation to the metamorphic history of some amphibolites and granulites. *American Jounal of Science* **264**, 526-542

Hames, WE, Tracy RJ, and Bodnar RJ (1989) Postmetamorphic unroofing history deduced from fluid inclusions, thermochronology, and thermal modeling: An example from southwestern New Englang. *Geology* **17**, 727-730

Jamtveit, B, Putnis C.V., and Malthe-Sorenssen A. (2009) Reaction induced fracturing during replacement processes. *Contrib Mineral Petrol* **157,** 127-133.

Kelemen, P.B. and Matter, J. (2008) In situ carbonation of peridotite for CO_2 storage. *PNAS U.S.A*. **105**, 17295-300.

Lackner, K.S. (2002) Carbonate chemistry for sequestering fossil carbon. *Annual Review of Energy and the Environment* **27**, 193-232.

Pacala, S.W. (2003) Global constraints on reservoir leakage. *Greenhouse Gas Control Technologies* **1-2**, 267-272.

Putnis A. (2002) Mineral replacement reactions; from macroscopic observations to microscopic mechanisms. *Mineral. Mag*. **66**, 689-708.

Putnis, A, and Putnis C. V. (2007) The mechanism of reequilibration of solids in the presence of a fluid phase. *Journal of Solid State Chemistry* **180**, 1783-1786

Putnis A. and John T. (2010) Replacement processes in the Earth's crust. *Elements* **6**, 159-164.

Schumacher, J.C and Schumacher, R (1989) Acadian metamorphism in central Massachusetts and south-western New Hampshire: evidence for contrasting P-T trajectories. *The Geological Society* **43**, 453-460

Sheppard, M.C. and Socolow, R.H. (2007) Sustaining fossil fuel use in a carbon-constrained world by rapid commercialization of carbon capture and sequestration. *Aiche Journal* **53 12**, 3022-3028.

Thomson, J. (2001) A counterclockwise P+-T path for anatectic pelites, south-central Massachusetts: *Contrib Mineral Petrol* **141**, 623-641

Winslow, D.M., Bodnar R.J, and Tracy R.J. (1994) Fluid inclusion evidence for an anticlockwise metamorphic P-T path in central Massachusetts. *Journal of Metamorphic Geology* **12,** 361-371